CHOROIDAL NEVUS IMAGING FEATURES IN 3,806 CASES AND RISK FACTORS FOR TRANSFORMATION INTO MELANOMA IN 2,355 CASES

The 2020 Taylor R. Smith and Victor T. Curtin Lecture

CAROL L. SHIELDS, MD, LAUREN A. DALVIN, MD, DAVID ANCONA-LEZAMA, MD, MICHAEL D. YU, BS, MAURA DI NICOLA, MD, BASIL K. WILLIAMS, JR., MD, J. ANTONIO LUCIO-ALVAREZ, MD, SU MAE ANG, BS, SEAN MALONEY, BS, R. JOEL WELCH, MD, JERRY A. SHIELDS, MD

Purpose: To use multimodal imaging for identification of risk factors for choroidal nevus transformation into melanoma.

Methods: Retrospective chart review of 3806 consecutive choroidal nevi with imaging and 2355 choroidal nevi with additional follow up to identify factors predictive of transformation of choroidal nevus into melanoma.

Results: The median patient age was 62.5 years and Caucasian race in 3167 (95%). The choroidal nevus demonstrated median basal diameter of 4.0 mm and thickness of 1.4 mm. Imaging included optical coherence tomography (OCT) showing subretinal fluid (SRF) in 312 (9%), ultrasonography (US) with acoustic hollowness in 309 (9%), and hyperautofluorescence (AF) in 100 (3%). Of those 2355 choroidal nevi with follow up, Kaplan-Meier estimates of nevus transformation into melanoma at 1, 5, and 10 years were 1.2%, 5.8%, and 13.9%, respectively. Multivariate analysis, using multimodal imaging for detection of factors predictive of nevus transformation into melanoma, included thickness >2 mm on US (hazard ratio (HR) 3.80, $p < 0.0001$), SRF on OCT as cap over nevus (HR 3.00, $p < 0.0001$) or SRF ≤ 3 mm from nevus margin (HR 3.56, $p = 0.0003$), symptomatic vision loss $\leq 20/50$ on Snellen visual acuity (VA) (HR 2.28, $p = 0.005$), orange pigment (lipofuscin) hyperautofluorescence on AF (HR 3.07, $p = 0.0004$), acoustic hollowness on US (HR 2.10, $p = 0.0020$), and tumor diameter >5 mm on photography (HR 1.84, $p = 0.0275$). These factors can be recalled by the mnemonic "To Find Small Ocular Melanoma Doing IMaging" (TFSOM-DIM) representing Thickness >2 mm (US), Fluid subretinal (OCT), Symptoms vision loss (VA), Orange pigment (AF), Melanoma hollow (US), and DIaMeter >5mm (photography). The mean 5-year estimates of nevus growth into melanoma were 1% (HR 0.8) for those with 0 risk factor, 11% (HR 3.09) with 1 factor, 22% (HR 10.6) with 2 factors, 34% (HR 15.1) with 3 factors, 51% (HR 15.2) with 4 factors, 55% (HR 26.4) with 5 risk factors, and not-estimable with all 6 risk factors.

Conclusion: In this analysis, multimodal imaging was capable of detecting risk factors for nevus transformation into melanoma, including thickness >2 mm (US), fluid subretinal (OCT), symptoms vision loss (Snellen acuity), orange pigment (AF), melanoma hollowness (US), and diameter >5 mm (photography). Increasing number of risk factors imparts greater risk for nevus transformation into melanoma, including thickness >2 mm (US), fluid subretinal (OCT), symptoms vision loss (Snellen acuity), orange pigment (AF), melanoma hollowness (US), and diameter >5 mm (photography). Increasing number of risk factors imparts greater risk for transformation.

RETINA 39:1840–1851, 2019

Clinical factors for early detection of cancer, particularly cutaneous and uveal melanoma, have been identified.[1–17] These factors are based on sentinel signs predictive of transformation of a precursor lesion (nevus) into a malignancy (melanoma). An easily recalled mnemonic can aid in the appraisal of risk factors for malignant transformation.[2,4,7–11] For example, the ABCDE criteria for cutaneous melanoma (asymmetry, border irregularity, color variegation, diameter >6 mm, and evolution) have led to earlier detection of melanoma at a thinner state, which typically translates to improved prognosis.[8,12,13] Before this lettering, cutaneous melanoma was often detected at a late stage, when the tumor was nodular, ulcerated, or bleeding, and prognosis was poor.[14] In the 1980s, a team of experienced dermatologists at New York University developed the objective, reproducible lettering based on a cooperative group database and provided a simple algorithm for early detection.[15] Later, in the 1990s, technological advances with dermoscopy (epiluminescence microscopy), digital image analysis, and image recognition via visible and nonvisible wavelengths were explored for improved detection.[16] The importance of early detection of cutaneous melanoma is underscored, especially when recognizing that tumor detection at <1 mm correlates with 5-year survival of 94% compared with >4-mm thickness with only 49% survival.[8] In fact, physician-detected melanoma (mean, 0.40-mm thickness) is typically far thinner than patient-detected (mean, 1.17 mm) or spouse-detected (mean, 1.00 mm) melanoma.[11,12] In addition, most skin melanoma is currently discovered by full-body skin examination, not by patient complaint, and more likely represents melanoma in situ.[12]

Table 1. Choroidal Nevus Transformation Into Melanoma Using Multimodal Imaging in 3,806 Nevi of 3,584 Eyes in 3,334 Patients: Patient Demographics

Demographic Features	Total (n = 3,806 Tumors, 3,584 Eyes, 3,334 Patients), n (%)
Age (years), mean (median, range) (n = 3,334 patients)	60.8 (62.5, 0.1–101.5)
Race (n = 3,334 patients)	
White	3,167 (95)
African American	27 (1)
Hispanic	38 (1)
Asian	13 (<1)
Other/unknown	89 (3)
Gender (n = 3,334 patients)	
Male	1,263 (38)
Female	2,071 (62)
Cutaneous disease (n = 3,334 patients)	
Dysplastic nevus syndrome	5 (<1)
Skin melanoma	156 (5)
Neurofibromatosis	4 (<1)
Ocular history (n = 3,334 patients)	
Ocular melanocytosis	41 (1)
Uveal melanoma	90 (3)
Fellow eye	74 (2)
Same eye	26 (1)
Visual acuity (n = 3,584 eyes)	
≤20/40	3,215 (90)
20/50–20/100	283 (8)
≥20/200	74 (2)

Data are collected per unique patient except visual acuity, which is collected per unique eye.

Similarly, identification of choroidal nevus[18–21] at risk of transformation into melanoma has evolved over the past 40 years from arbitrary ophthalmoscopic labeling of suspicious versus nonsuspicious nevus, to more objective criteria of tumor thickness >2 mm, presence of subretinal fluid, symptoms of photopsia, floaters, or vision loss, overlying orange pigment, and tumor margin ≤3 mm of the optic disk, remembered with the mnemonic TFSOM representing "*to find small ocular melanoma*."[2,3] Later, analysis of a larger cohort led to the addition of risk factors including ultrasonographic hollowness, halo absence, and drusen absence, and a revision in the mnemonic to "*to find small ocular melanoma—using helpful hints daily*" was made.[4,5] In these studies, most of the risk factors were determined clinically on ophthalmoscopy, without the benefit of multimodal imaging.

In recent years, multimodal imaging has been used in ocular oncology with improved tumor diagnosis and understanding. Imaging techniques

From the Ocular Oncology Service, Wills Eye Hospital, Thomas Jefferson University, Philadelphia, Pennsylvania.

Supported in part by the Eye Tumor Research Foundation, Philadelphia, PA (C.L.S.), an unrestricted grant from Research to Prevent Blindness, Inc, New York, NY (L.A.D.), the Heed Ophthalmic Foundation, San Francisco, CA (L.A.D.), a grant from the VitreoRetinal Surgery Foundation Minneapolis, MN (L.A.D.), and a grant from Aura Bioscience Incorporated, Cambridge, MA (C.L.S.). The funders had no role in the design and conduct of the study, in the collection, analysis, and interpretation of the data, and in the preparation, review, or approval of the manuscript. C. L. Shields has had full access to all the data in the study and takes responsibility for the integrity of the data and the accuracy of the data analysis.

Presented in part as the Taylor R. Smith/Victor T. Curtin Lecture, Aspen Retina Detachment Society, Aspen, CO, March 3, 2020 (C.L.S.).

None of the authors has any financial/conflicting interests to disclose.

Rishita Nutheti, PhD, provided statistical analysis.

Reprint requests: Carol L. Shields, MD, Ocular Oncology Service, 840 Walnut Street, Suite 1440, Philadelphia, PA 19107; e-mail: carolshields@gmail.com

Table 2. Choroidal Nevus Transformation Into Melanoma Using Multimodal Imaging in 3,806 Nevi of 3,584 Eyes in 3,334 Patients: Tumor Features

Tumor Features	Total (n = 3,806 Tumors, 3,584 Eyes, 3,334 Patients), n (%)
Involved eye (n = 3,334 patients)	
Right	1,618 (49)
Left	1,466 (44)
Both	250 (7)
Symptoms (n = 3,334 patients)	
Decreased visual acuity	218 (6)
Visual field defect	42 (1)
Flashes and floaters	190 (5)
No symptoms	3,122 (87)
No. of nevi (n = 3,584 eyes)	
Per patient, mean (median, range)	1 (1, 1–10)
Per eye, mean (median, range)	1 (1, 1–6)
1	3,248 (91)
2	270 (8)
3	43 (1)
≥4	11 (<1)
Quadrantic location (n = 3,806 nevi)	
Macula	1,044 (27)
Inferior	752 (20)
Temporal	662 (17)
Superior	794 (21)
Nasal	554 (15)
Anteroposterior location (n = 3,806 nevi)	
Macula	1,061 (28)
Macula to equator	2,301 (60)
Equator to ora serrata	444 (12)
Proximity to the optic disk (mm) (n = 3,806 nevi), mean (median, range)	5.2 (5, 0–23)
Proximity to the foveola (mm) (n = 3,806 nevi), mean (median, range)	4.9 (4, 0–20)
Largest basal diameter (mm) (n = 3,806 nevi), mean (median, range)	4.6 (4, 0.1–20)
Thickness (mm) (n = 3,806 nevi), mean (median, range)	1.5 (1.4, 0.1–6.7)
Color (n = 3,806 nevi)	
Pigmented	3,202 (84)
Nonpigmented	347 (9)
Mixed	257 (7)
Halo nevus (n = 3,806 nevi)	244 (6)

Table 3. Choroidal Nevus Transformation Into Melanoma Using Multimodal Imaging in 3,806 Nevi of 3,584 Eyes in 3,334 Patients: Multimodal Imaging Features

Imaging Features	Total (n = 3,806), n (%)
OCT (n = 3,428 nevi)	
Subretinal fluid	
Overlying nevus	172 (5)
<3 mm from margin	110 (3)
3–6 mm from margin	25 (1)
>6 mm from margin	5 (<1)
Retinal invasion	5 (<1)
Retinal edema over nevus	139 (4)
Drusen	1,524 (44)
RPE atrophy	409 (12)
RPE hyperplasia	143 (4)
RPE fibrous metaplasia	189 (6)
RPED over nevus	113 (3)
Choroidal neovascularization over nevus	30 (1)
Surface configuration	
Dome	1,912 (56)
Lumpy bumpy	38 (1)
Excavated	26 (1)
Flat	1,452 (42)
Location within the choroid	
Inner	754 (22)
Outer	1,859 (54)
Full thickness	636 (19)
Not assessable	179 (5)
AF (n = 3,649 nevi)	
Orange pigment	100 (3)
RPE trough	103 (3)
US (n = 3,444 nevi)	
Flat configuration	2,290 (66)
Dome configuration	1,154 (34)
Hollow echogenicity	309 (9)
Dense echogenicity	3,135 (91)

RPED, retinal pigment epithelial detachment.

include optical coherence tomography (OCT),[22–25] fundus autofluorescence (AF),[26,27] and high-resolution ultrasonography (US). These modalities allow for subclinical detection of subretinal fluid, photoreceptor loss, intraretinal edema, lipofuscin (orange) pigment, and acoustic internal tumor qualities, often not visible with ophthalmoscopy alone. In this analysis, we explore, for the first time in the published literature, risk factors using multimodal imaging of choroidal nevus in 3,806 cases for early detection of choroidal melanoma.

Methods

A retrospective chart review was performed on all patients with the clinical diagnosis of choroidal nevus managed on the Ocular Oncology Service at Wills Eye Hospital between January 1, 2007, and January 1, 2017. This 10-year period did not overlap previous studies[2–4] on risk factors for choroidal nevus, and there was no patient in this series that

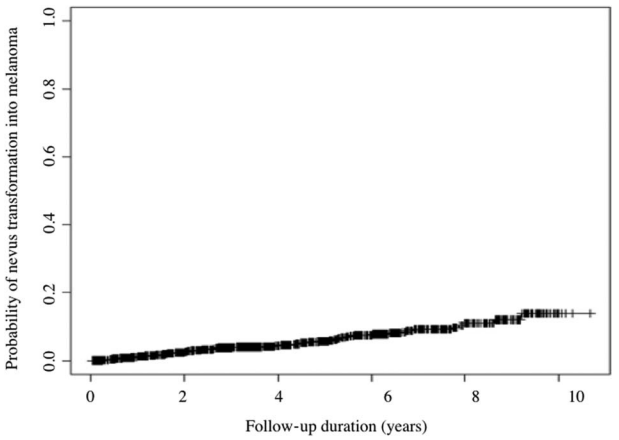

Fig. 1. Kaplan–Meier estimates for time of choroidal nevus transformation into melanoma in 3,806 cases.

was included in previous similar studies.[2–4] This study was approved by the Institutional Review Board/Ethics Committee of Wills Eye Hospital and adhered to the tenets of the Declaration of Helsinki and Health Insurance Portability and Accountability Act.

All patients were examined by one of the senior authors (C.L.S. or J.A.S.) using techniques of slit-lamp biomicroscopy and indirect ophthalmoscopy of the fundus. Clinical findings of the choroidal nevus were recorded on large fundus drawings in all cases. Data at initial examination included patient age, race, sex, medical history, ocular melanocytosis, involved eye, symptoms, and best-corrected visual acuity by Snellen and logMAR methods. The choroidal nevus was quantified as to total number per patient and per eye. The nevus features included quadrantic location of tumor epicenter (inferior, temporal, superior, nasal, and macula), anteroposterior epicenter location (macula, macula to equator, and equator to ora serrata), distance of tumor margin to the optic disk and foveola (mm), largest tumor basal dimension and thickness (mm), tumor color (pigmented, mixed, and nonpigmented), and presence of clinically evident subretinal fluid, orange pigment, drusen, halo, retinal pigment epithelial

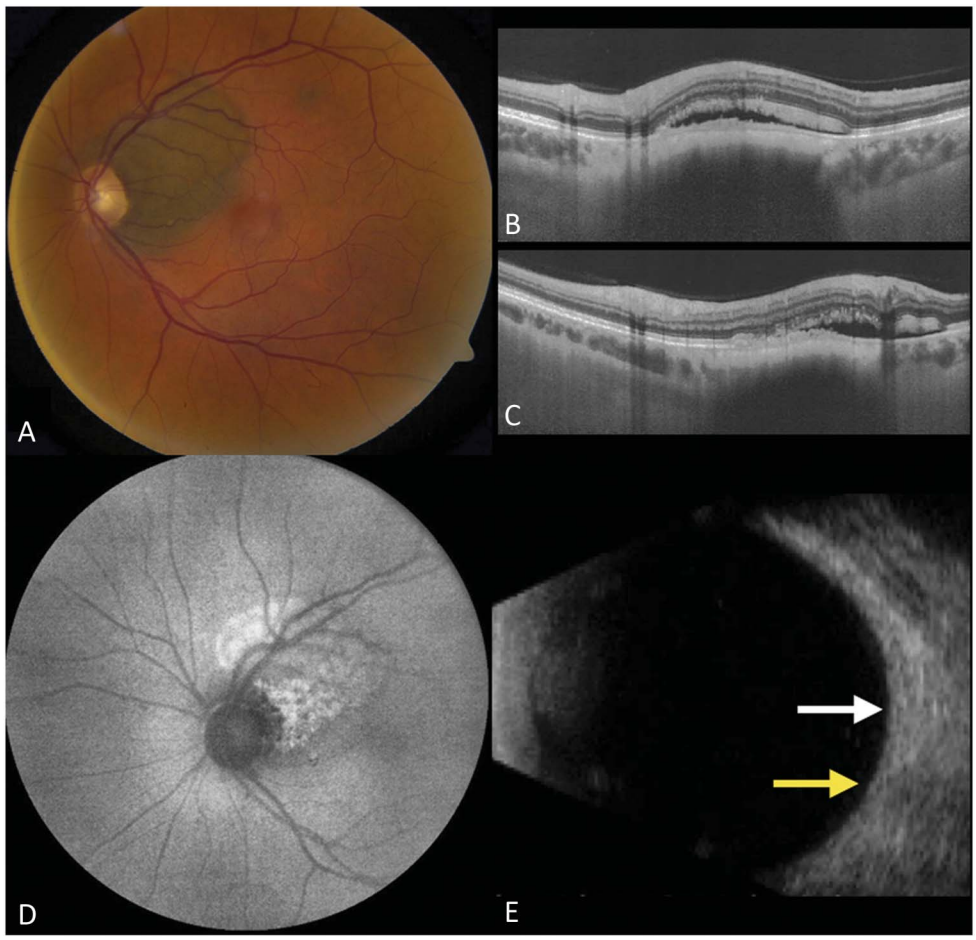

Fig. 2. A. High-risk juxtapapillary choroidal nevus with overlying subretinal fluid, confirmed as a cap on (**B**) horizontal and (**C**) as ≤3 mm from lesion on vertical OCT. There was overlying orange lipofuscin, demonstrated on (**D**) AF. **E.** Ultrasonography shows a flat lesion (white arrow) of 1.6-mm thickness immediately superior to the optic nerve (yellow arrow).

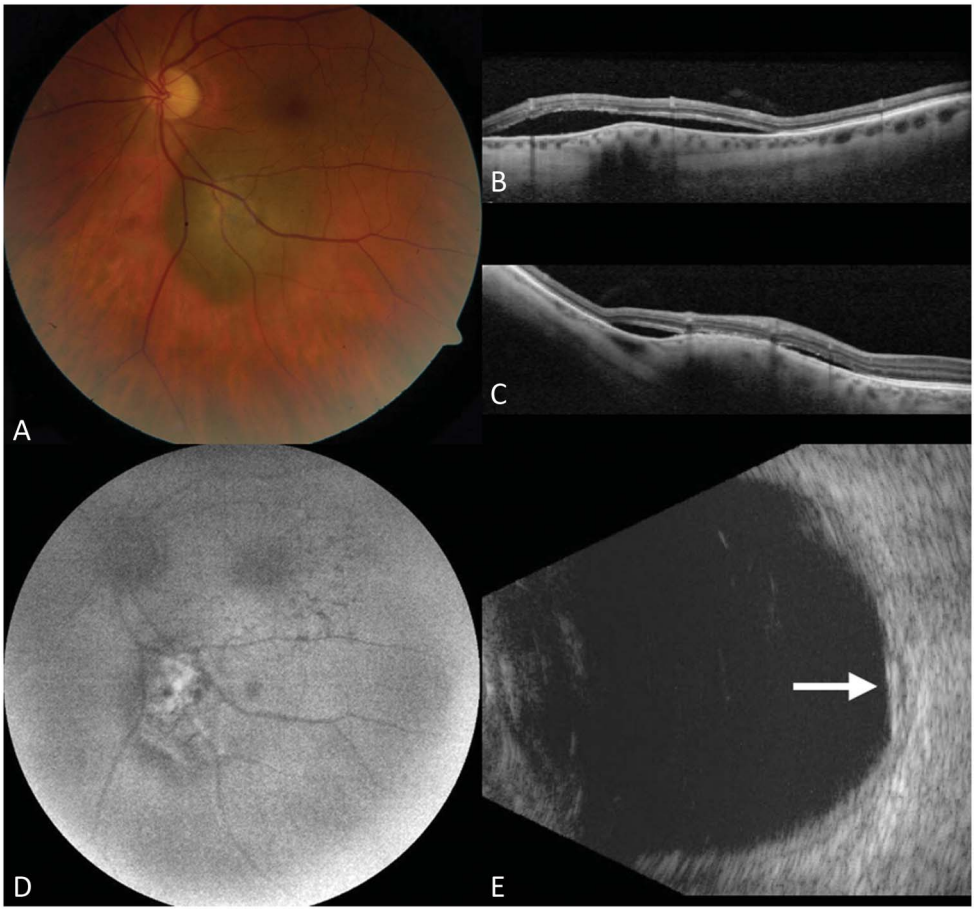

Fig. 3. A. High-risk dome-shaped choroidal nevus with overlying subretinal fluid, confirmed as a cap on (**B**) horizontal and ≤3 mm thickness on (**C**) vertical OCT. There was overlying orange lipofuscin, demonstrated on (**D**) AF. **E.** Ultrasonography shows a dome-shaped, acoustically hollow lesion (white arrow) of 2.3-mm thickness.

(RPE) alterations, retinal invasion, and choroidal neovascular membrane. If an eye had more than one nevus, nevi smaller than 1 mm in basal diameter and thickness were excluded from the analysis.

Multimodal imaging included fundus photography, spectral domain OCT, fundus AF, and ocular US. The OCT used enhanced depth imaging technology and was performed through a dilated pupil (Heidelberg Spectralis HRAOCT; Heidelberg Engineering, Heidelberg, Germany) using accompanying acquisition and analysis software (version 5.3.3.0 with automated enhanced depth imaging), as indicated in the previous study.[24] The axial resolution was 3.5 μm, with an imaging speed of 40,000 A-scans per second. The images were captured using a custom image acquisition protocol of up to 13 raster lines of 9-mm image length, with 1,536 A-scans per line. The OCT findings included the presence of subretinal fluid and location of the fluid relative to the nevus with angle of elevation of fluid and status of photoreceptors, foveola, drusen, retinal edema, and retinal invasion. Additional OCT features regarding the RPE (atrophy, hyperplasia, fibrous metaplasia, and detachment) and the presence of choroidal neovascularization were recorded. The OCT features of the nevus included surface configuration, precise location in the choroid (inner, outer, or full thickness), internal qualities (homogeneous or heterogeneous), tumor shadowing, scleral bowing, and estimated thickness. The fundus AF was performed with special filters (580-nm excitation, 695-nm barrier filter) to avoid imaging the AF of the crystalline lens using a Zeiss camera (Carl Zeiss Meditec Inc, Jena, Germany) and Ophthalmic Imaging Systems (Sacramento, CA) software, as previously recorded.[27] The AF features included presence, extent, and location (over nevus, dispersed, or settled in subretinal fluid) of hyperautofluorescence (lipofuscin) and hypoautofluorescence findings. Ultrasonography was performed using standard A-scan and B-scan imaging of the intraocular mass, with a coupling agent using Sonomed Escalon (Wayne, PA) or Eye Cubed (Ellex, Adelaide, Australia) technology. The US findings included B-scan tumor configuration and acoustic quality, and A-scan internal reflectivity.

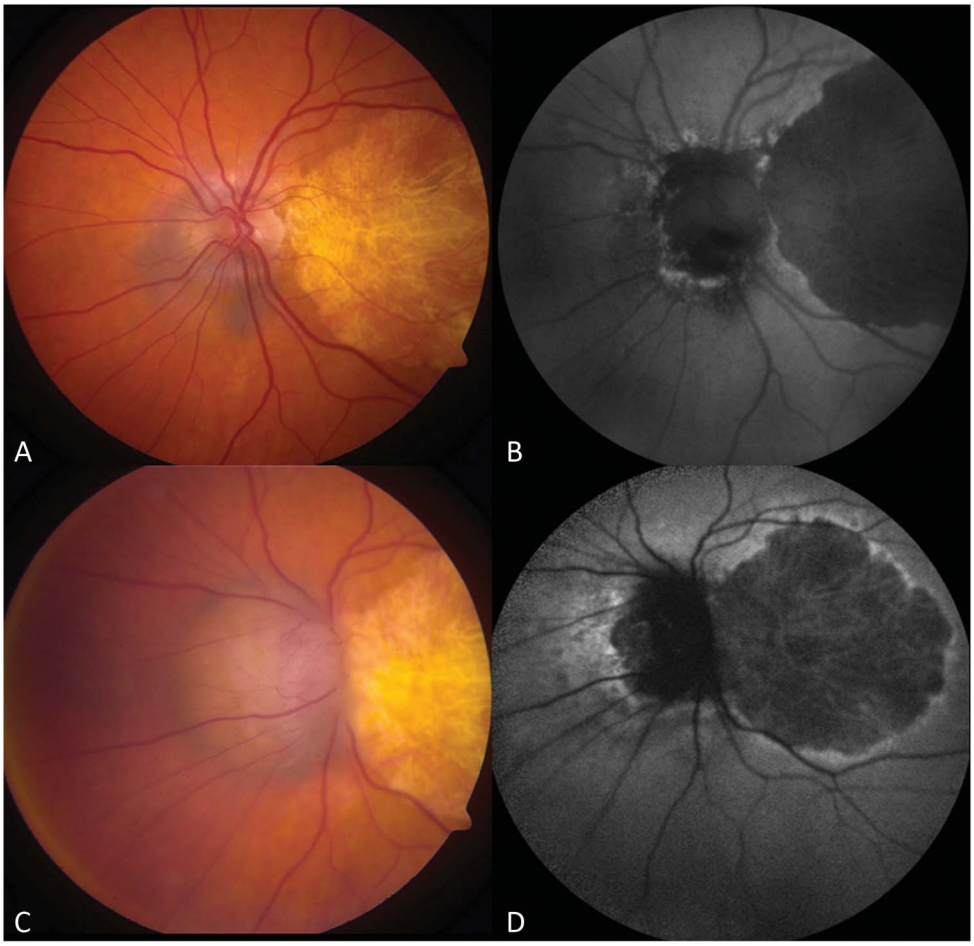

Fig. 4. A. Flat choroidal nevus with overlying orange pigment, confirmed on (**B**) AF and with trace subretinal fluid. Note the geographic atrophy secondary to macular degeneration in this 90-year-old patient. **C.** After 1 year of observation, transformation into a nodular choroidal melanoma was noted, overhanging the optic disk, and with surrounding shallow subretinal fluid on the nasal side noted as (**D**) diffuse hyperautofluorescence.

Statistical Analysis

The nevus was then analyzed longitudinally with regard to a single clinical outcome of transformation (growth) into melanoma, classified as enlargement in basal dimension or thickness by at least 0.5 mm (arbitrary) over a short time period. Only nevi with available follow-up were included in this analysis. All data were tabulated using Microsoft Excel 2016 version 15.24 (Microsoft Corp, Redmond, WA), which summarized the demographics, tumor features, and imaging features of all nevi. The hazard ratio (HR), 95% confidence intervals, and *P* value were calculated using Cox regression analysis. A *P* value <0.05 was considered statistically significant.

Kaplan–Meier estimates were calculated for time to growth into melanoma. A series of univariate Cox regression analyses were performed to identify the factors predictive of growth into melanoma based on clinical and imaging features at presentation. All variables were analyzed as discrete variables. Subsequent multivariate analyses were performed using the Cox proportional hazard model forward stepwise method for the factors identified to be significant at the 5% level of significance. Hazard ratios were calculated for each risk factor and the number of risk factors. All significant analysis was performed using SAS 13.2 version.

Results

There were 3,334 patients with 3,806 choroidal nevi in this 10-year study from 2007 to 2017. Of those 2,075 patients with follow-up, there were 2,355 choroidal nevi. The mean follow-up was 3 years (median 3, range <1–11 years). The demographic features are listed in Table 1. The mean patient age was 60.8 years (median 62.5, range 0.01–101.5 years). There was predominance of whites (95%), women (62%), and visual acuity ≤20/40 (90%).

The tumor features are listed in Table 2. Symptoms per eye included decreased visual acuity (6%), flashes/floaters (5%), visual field defect (1%), and no

Table 4. Choroidal Nevus Transformation Into Melanoma Using Multimodal Imaging in 2,355 Tumors of 2,211 Eyes in 2,075 Patients: Growth With Nevus Transformation Into Melanoma in 90 Cases

Growth Features	Total (n = 90), n (%)
Absolute growth (mm)	
Basal diameter, mean (median, range)	2.4 (2.0, 0.0–8.0)
Thickness, mean (median, range)	1.1 (0.8, 0.0–5.7)
Growth rate (mm/year)	
Basal diameter, mean (median, range)	1.0 (0.4, 0.0–8.0)
Thickness, mean (median, range)	0.5 (0.2, 0.0–3.8)
OCT	
Increase in SRF	57 (63)
Increase in drusen	3 (3)
AF	
Increase in orange pigment	36 (40)
US	
Increase in acoustic hollowness	27 (30)

SRF, subretinal fluid.

Table 5. Choroidal Nevus Transformation Into Melanoma Using Multimodal Imaging in 2,355 Cases Using Kaplan–Meier Estimates

	Total (n = 2,355)	
Year	Kaplan–Meier Estimates (%)	No. Failed/Left
1	1.2 ± 0.2	25/1,725
3	3.8 ± 0.5	59/916
5	5.8 ± 0.7	72/477
7	9.3 ± 1.2	85/226
10	13.9 ± 2.6	90/4

symptoms were found in 3,122 (87%) eyes. The mean tumor diameter was 4.6 mm (median 4, range 1–20 mm) and mean thickness was 1.5 mm (median 1.4, range 0.1–6.7 mm). Most nevi were located in the zone between the macula and equator (60%), and a surrounding halo (6%) was noted.

The imaging features are listed in Table 3. By using OCT, subretinal fluid was noted overlying the nevus (5%), <3 mm from margin (3%), and >3 mm from margin (1%). There were overlying retinal edema (4%), drusen (44%), RPE detachment (3%), and choroidal neovascularization (1%). The choroidal nevus was located in the inner (22%), outer (54%), or full-thickness (19%) choroid. By using AF, overlying orange lipofuscin pigment (3%) was detected. By using US, the tumor showed flat configuration (66%) and dense echogenicity (91%). All patients had fundus photography (Table 2).

There were 90 (2.4%) choroidal nevi to demonstrate growth into melanoma (Figures 1–4), and the features are listed in Table 4. The absolute growth (growth rate) was a mean of 2.4 mm diameter (1.0 mm/year) and 1.1 mm thickness (0.5 mm/year). During the period of growth, there was an increase in subretinal fluid (63%) on OCT, increase in orange pigment (40%) on AF, and increase in acoustic hollowness (30%) on US.

The Kaplan–Meier estimates for transformation of nevus into melanoma are listed in Table 5. Transformation was detected in 1.2% at 1 year, 5.8% at 5 years, and 13.9% at 10 years.

The clinical and imaging features predictive of growth into melanoma are listed in Table 6 (univariate analysis) and Table 7 (multivariate analysis). In multivariate analysis, the most important factors for transformation into melanoma included Thickness >2 mm (US), subretinal Fluid (OCT), Symptoms of visual acuity loss to 20/50 or worse (Snellen acuity), Orange pigment (AF), Melanoma acoustic hollowness (US), and tumor DIaMeter >5 mm (photography). These factors can be recalled by the mnemonic "To Find Small Ocular Melanoma Doing IMaging" (TFSOMDIM). The mean 5-year estimates for growth of nevus into melanoma were 1.1% (HR 0.8) for those with 0 risk factor, 11% (HR 3.09) with 1 factor, 22% (HR 10.6) with 2 factors, 34% (HR 15.1) with 3 factors, 51% (HR 15.2) with 4 factors, 55% (HR 26.4) with 5 risk factors, and not estimable with all 6 risk factors (Table 8).

Discussion

There have been several studies on the topic of choroidal nevus and risks of transformation into melanoma.[2–6,17,18] In 1994, Butler et al studied 293 "indeterminate pigmented choroidal tumors" of which 98 (33%) demonstrated growth.[17] These authors identified factors for growth; however, the study group of "indeterminate pigmented choroidal tumors" was arbitrarily selected based on "tumors [that] were large enough that we did not believe they were nevi, yet they appeared small enough (generally <10 mm in largest diameter and <3 mm in thickness) and inactive (based on minimal symptoms, good vision, and the absence of subretinal fluid) that we initially chose to follow them without intervention."[17] Subjective inclusion factors can limit real-world applicability.

In 1995, Shields et al[2] retrospectively studied a cohort of 1,329 consecutive patients, including all choroidal melanocytic tumors objectively measuring ≤3 mm in thickness by using US. These authors found five risk factors for growth into melanoma including increasing tumor thickness, subretinal fluid, symptoms, orange pigment, and tumor margin near the optic disk. The most important factor was increasing

Table 6. Choroidal Nevus Transformation Into Melanoma Using Multimodal Imaging in 2,355 Cases of 2,211 Eyes of 2,075 Patients: Univariate Analysis of Factors at Initial Presentation Predictive of Growth Into Melanoma

	Combined (n = 2,355)			
Variable	Growth Into Melanoma (n = 90), m (%)	No Growth Into Melanoma (n = 2,265), m (%)	HR (95% CI)	*P*
Sex, male vs. female	33 (37)	839 (37)	1.10 (0.72–1.70)	0.6522
Visual acuity, 20/50 or worse vs. better	15 (17)	186 (8)	2.66 (1.53–4.64)	*0.0006*
Symptoms				
Decreased vision vs. none	12 (13)	115 (5)	3.70 (2.00–6.84)	*<0.0001*
Visual field defect vs. none	0	29 (1)	0 (NE)	0.9780
Flashes/floaters vs. none	7 (8)	110 (5)	2.44 (1.12–5.32)	*0.0254*
Quadrantic location of nevus				
Inferior vs. macula	16 (18)	462 (20)	1.15 (0.59–2.23)	0.6832
Superior vs. macula	20 (22)	476 (21)	1.41 (0.75–2.65)	0.2800
Temporal vs. macula	22 (24)	384 (17)	1.69 (0.92–3.13)	0.0933
Nasal vs. macula	13 (14)	328 (14)	1.32 (0.65–2.68)	0.4385
Anteroposterior location				
Macula to the equator vs. macula	56 (62)	1,372 (61)	1.30 (0.78–2.17)	0.3100
Equator to the ora serrata vs. macula	14 (16)	260 (11)	1.53 (0.77–3.04)	0.2205
Distance of nevus to the optic nerve				
0 mm vs. >0 mm	14 (16)	205 (9)	1.63 (0.92–2.89)	0.0921
≤3 mm vs. >3 mm	30 (33)	860 (38)	0.83 (0.53–1.28)	0.3939
Distance of nevus to the foveola				
0 mm vs. >0 mm	9 (10)	146 (6)	1.53 (0.77–3.05)	0.2274
≤3 mm vs. >3 mm	38 (42)	1,008 (44)	0.87 (0.57–1.32)	0.5020
Largest basal dimension				
>5 mm vs. ≤5 mm	66 (73)	778 (34)	5.01 (3.14–8.00)	*<0.0001*
Thickness				
>2 mm vs. ≤2 mm	59 (66)	342 (15)	10.82 (7.00–16.7)	*<0.0001*
Color				*<0.0001*
Mixed vs. pigmented	22 (24)	209 (9)	2.91 (1.79–4.73)	0.9676
Nonpigmented vs. pigmented	5 (6)	155 (7)	0.98 (0.40–2.44)	
Halo, present vs. absent	7 (8)	157 (7)	1.12 (0.52–2.43)	0.7716
OCT				
Subretinal fluid (SRF)				
Cap vs. none	24 (27)	102 (5)	7.85 (4.81–12.8)	*<0.0001*
≤3 mm from nevus vs. none	13 (15)	60 (3)	9.73 (5.26–18.0)	*<0.0001*
3–≤6 mm vs. none	1 (1)	19 (1)	2.11 (0.29–15.3)	0.4613
>6 mm vs. none	1 (1)	4 (<1)	11.5 (1.59–83.7)	*0.0156*
Estimate SRF over nevus (μm)				
50–150 vs. <50	22 (24)	92 (4)	6.36 (3.92–10.3)	*<0.0001*
>150 vs. <50	4 (4)	38 (2)	4.21 (1.53–11.6)	*0.0054*
Angle of retina elevation from SRF				
10–30 vs. <10	18 (46)	86 (47)	1.05 (0.55–1.98)	0.8867
>30 vs. <10	1 (3)	6 (3)	5.82 (0.71–47.6)	0.1005
Photoreceptor status if SRF				
Shaggy vs. retracted	20 (53)	79 (44)	1.11 (0.57–2.18)	0.7581
Retracted vs. absent	15 (39)	17 (9)	1.44 (0.42–4.98)	0.5667
Shaggy vs. absent	20 (53)	79 (44)	1.60 (0.47–5.38)	0.4494
Drusen, present vs. absent	44 (50)	933 (44)	1.19 (0.79–1.81)	0.4105

(*continued on next page*)

Table 6. (*Continued*)

Variable	Combined (n = 2,355)			
	Growth Into Melanoma (n = 90), m (%)	No Growth Into Melanoma (n = 2,265), m (%)	HR (95% CI)	*P*
Retinal edema over nevus, present vs. absent	10 (11)	85 (4)	3.18 (1.64–6.14)	*0.0006*
RPE atrophy, present vs. absent	23 (26)	247 (12)	2.38 (1.48–3.83)	*0.0004*
RPE hyperplasia, present vs. absent	10 (11)	91 (4)	2.95 (1.53–5.71)	*0.0013*
RPE fibrous metaplasia, present vs. absent	9 (10)	113 (5)	1.88 (0.94–3.75)	0.0727
RPED over nevus, present vs. absent	2 (2)	68 (3)	1.46 (0.36–5.92)*	0.5980
Retinal invasion, present vs. absent	1 (1)	3 (<1)	4.10 (0.57–29.7)	0.1620
CNVM, present vs. absent	2 (2)	14 (<1)	3.72 (0.91–15.1)	0.0667
Surface configuration of nevus				
Dome vs. flat	79 (90)	1,132 (54)	7.56 (3.65–15.6)	*<0.0001*
Lumpy bumpy vs. dome	1 (1)	25 (1)	4.33 (0.54–34.7)	0.1670
Excavated vs. dome	0	15 (1)	0 (0 – NE)	0.9816
Location in the choroid of nevus				
Outer vs. inner	50 (63)	1,142 (57)	6.85 (2.14–22.0)	*0.0012*
Full thickness vs. outer	27 (34)	395 (20)	1.36 (0.85–2.17)	0.2010
Full thickness vs. inner	27 (34)	395 (20)	9.30 (2.82–30.7)	*0.0002*
Vascular compression, present vs. absent	44 (77)	789 (48)	3.33 (1.79–6.18)	*0.0001*
Internal qualities of nevus, heterogenous vs. homogenous	56 (70)	1,379 (67)	1.09 (0.68–1.76)	0.7185
Shadowing				
Moderate vs. minimal	55 (71)	1,270 (64)	2.70 (1.29–5.68)	*0.0086*
Maximal vs. minimal	15 (19)	205 (10)	4.28 (1.81–10.1)	*0.0009*
Scleral bowing, present vs. absent	9 (13)	142 (8)	1.68 (0.83–3.38)	0.1464
Foveolar status				
SRF vs. normal	4 (5)	25 (1)	4.56 (1.67–12.5)	*0.0032*
Edema vs. normal	2 (2)	8 (<1)	11.5 (2.80–47.0)	*0.0007*
Atrophy vs. normal	2 (2)	4 (<1)	10.9 (2.67–44.4)	*0.0009*
AF				
Orange pigment, present vs. absent	16 (18)	60 (3)	7.84 (4.56–13.5)	*<0.0001*
Orange pigment extent				
25%–50% vs. <25%	7 (8)	13 (1)	2.75 (0.87–8.70)	0.0843
50%–75% vs. <25%	2 (2)	4 (<1)	2.47 (0.46–13.2)	0.2898
>75% vs. <25%	1 (1)	2 (<1)	4.48 (0.51–39.1)	0.1755
RPE trough, present vs. absent	9 (10)	69 (3)	3.90 (1.95–7.78)	*0.0001*
US				
Configuration, dome vs. flat	69 (78)	700 (33)	6.63 (4.03–10.9)	*<0.0001*
Acoustic density, hollow vs. solid	37 (42)	182 (9)	6.64 (4.35–10.2)	*<0.0001*

*Absent vs. present. Values in italics are statistically significant.
CNVM, choroidal neovascular membrane; NE, not estimable; RPED, retinal pigment epithelial detachment.

Table 7. Choroidal Nevus Transformation Into Melanoma Using Multimodal Imaging in 2,355 Cases of 2,211 Eyes of 2,075 Patients: Multivariate Analysis of Factors at Initial Presentation Predictive of Growth Into Melanoma

				Total (n = 90/2,355)			Total (n = 90/2,355)	
Variable	Letter	Mnemonic	Representing	Feature Present, n (%)	Feature Absent, n (%)	HR (95% CI) Based on Feature Present/ Absent	HR (95% CI) by Multivariate Analysis	*P*
Thickness tumor >2 mm vs. ≤2 mm	T	To	Thickness >2 mm by US	59 (15)	31 (2)	3.82 (2.23–6.53)	3.80 (2.22–6.51)	<0.0001
Fluid subretinal Cap vs. none	F	Find	Fluid subretinal by OCT	37 (19)	51 (3)	3.11 (1.94–4.99)	3.00 (1.77–5.09)	<0.0001
≤3 mm from nevus vs. none							3.56 (1.78–7.12)	0.0003
Symptoms visual acuity loss 20/50 or worse vs. better	S	Small	Symptoms vision loss by Snellen	15 (7)	75 (3)	2.34 (1.33–4.11)	2.28 (1.28–4.04)	0.0050
Orange pigment Present vs. absent	O	Ocular	Orange pigment by AF	16 (21)	73 (3)	3.25 (1.80–5.89)	3.07 (1.65–5.74)	0.0004
Melanoma acoustic density Hollow vs. solid	M	Melanoma	Melanoma hollow by US	37 (17)	52 (3)	2.08 (1.30–3.32)	2.10 (1.31–3.37)	0.0020
Tumor diameter >5 mm vs. ≤5 mm	DIM	Doing IMaging	DIaMeter by photography	66 (8)	24 (2)	1.83 (1.06–3.15)	1.84 (1.07–3.17)	0.0275

Snellen, Snellen visual acuity.

thickness, imparting a relative risk for growth of 4.3 for slightly thick (1.1–2.0 mm) and 5.2 for moderately thick (2.1–3.0 mm) nevi, compared with thin (0–1.0 mm) tumors. Subretinal fluid (relative risk 1.4) and orange pigment (relative risk 1.5) carried the least relative risk in that study; however, that study was performed before spectral domain OCT and fundus AF were commercially available, and so they were not used for imaging in that study. Subsequent study on a larger cohort of 2,514 choroidal melanocytic tumors ≤3 mm revealed Kaplan–Meier growth into melanoma in 1.9% at 1 year, 8.6% at 5 years, and 12.8% at 10 years.[4] Similar risk factors were identified and two new factors were added including ultrasonographic hollowness and absence of the surrounding halo. Interestingly, the relative importance of subretinal fluid and orange pigment was greater with HR of 3.11 and 2.75, respectively, as attention to these factors was raised based on previous publication. In addition, time domain OCT and, in some cases, spectral domain OCT were available for improved detection of subretinal fluid, but AF was not available for most cases; so, judgement of orange pigment was by clinical examination alone.

Multimodal imaging is now an indispensable tool in ocular oncology for better definition of intraocular tumor features and surrounding tissue alterations. Currently, spectral domain OCT, fundus AF, and ocular US are routinely used to image choroidal nevus and melanoma.[22–27] The purpose of this analysis was to explore the role of multimodal imaging for detection of features that may signify nevi at risk of malignant transformation. In this analysis, we found six important factors for tumor growth by multivariate analysis, four of which were detected specifically using

Table 8. Choroidal Nevus Transformation Into Melanoma Using Multimodal Imaging in 2,355 Cases of 2,211 Eyes of 2,075 Patients: Kaplan–Meier 5-Year Estimates For Nevus Transformation Into Melanoma Using Multivariate Risk Factors

			Total (n = 90/2,355)			
Variable	Representing	Multimodal Imaging Modality	No. With Growth/ No. With Feature(s) (%)	No. With Growth/ No. Without Feature(s) (%)	Kaplan–Meier 5-Year Growth, %	HR For Growth at 5 Years (95% CI)
0 features				8/1,035 (0.8)	1%	0.08 (0.03–0.19)
1 feature				8/1,221 (0.7)	11%	3.09 (1.05–9.04)
T	Thickness >2 mm	US	59/401 (15)	31/1,955 (2)	26%	7.76 (4.32–13.9)
F	Fluid subretinal	OCT	37/199 (19)	51/1,992 (3)	27%	2.67 (1.58–4.52)
S	Symptoms VA ≤20/50	Snellen chart	15/201 (7)	75/2,155 (3)	9%	2.12 (1.10–4.05)
O	Orange pigment	AF	16/76 (21)	73/2,210 (3)	37%	3.16 (1.71–5.86)
M	Melanoma hollow	US	37/219 (17)	52/1,964 (3)	23%	2.06 (1.24–3.42)
DIM	DIaMeter >5 mm	Photography	66/844 (8)	24/1,512 (2)	12%	NS
2 features				20/1,841 (1)	22%	10.6 (4.97–22.7)
3 features				39/2,139 (2)	34%	15.1 (9.29–24.5)
4 features				69/2,296 (3)	51%	15.2 (8.99–25.7)
5 features				84/2,343 (4)	55%	26.4 (10.6–66.0)
6 features				90/2,355 (4)	NE	NE

NE, not estimable; NS, not significant.

multimodal imaging. These factors included Thickness >2 mm (by US), subretinal Fluid (by OCT), Symptoms of visual acuity loss of 20/50 or worse (by Snellen acuity), Orange pigment (by AF), Melanoma acoustic hollowness (by US), and tumor DIaMeter >5 mm (by photography). These factors can be recalled by the mnemonic "To Find Small Ocular Melanoma Doing IMaging" (TFSOM-DIM). The Kaplan–Meier estimates for growth and HR at 5 years were highest for each of the factors detected by multimodal imaging, including features of thickness >2 mm (by US) (26%, HR 7.76), subretinal fluid (by OCT) (27%, HR 2.67), orange pigment (by AF) (37%, HR 3.16), and acoustic hollowness (by US) (23%, HR 2.06). The remaining factors, detected by standard clinical examination, were less important, registering lower Kaplan–Meier 5-year estimates, including symptoms of vision loss (9%, HR 2.12) and tumor diameter >5 mm (12%, HR nonsignificant).

In a previous study,[4] the symptoms of flashes/floaters were significant in multivariate analysis. In this current analysis, these symptoms were significant in univariate analysis, but not in the multivariate analysis. This could be due to the greater importance of OCT-evident subretinal fluid herein, as this feature often manifests as flashes/floaters. This feature might not have been clinically detectable before the use of OCT in older reports.[4]

In previous analyses,[4,5] tumor margin ≤3 mm to the optic disk, absence of drusen, and absence of the surrounding halo were features predictive of nevus growth into melanoma, but these features did not reach significance in the multivariate analysis in this current study. By univariate analysis, of those 90 cases with nevus growth into melanoma, tumor location at 0 mm from the optic disk (vs. >0 mm from the disk), tumor location ≤3 mm from the disk (vs. >3 mm from the disk), surrounding halo (vs. no halo), and presence of drusen (vs. no drusen) were not significant factors.

The most profound risks of choroidal nevus growth into melanoma occurred with a combination of multivariate factors. For example, the 5-year Kaplan–Meier estimate of growth of nevus into melanoma in a tumor with no risk factor was 1% compared to those with 1 factor (11%), 2 factors (22%), 3 factors (34%), and 4 or more factors (>50%). Likewise, HR was 3.1 for 1 factor and increased to 10.6 for 2 factors, 15.1 for 3 factors, 15.2 for 4 factors, and 26.4 for 5 factors. Thus, the combination of factors provided robust predictive value.

There are limitations to this analysis. In this retrospective review of the 10-year experience using multimodal imaging in the assessment of 3,806 choroidal nevi, there have been changes, upgrades, and improvements in imaging quality. Furthermore, all patients underwent fundus photography, but not every nevus was imaged with all three of the other modalities of OCT, AF, and US. In this cohort,

multimodal imaging was advised in all cases and was available for review in 3,428/3,806 (90%) imaged with OCT, 3,649/3,806 (96%) imaged with AF, and 3,444/3,806 (90%) imaged with US.

In summary, we have evaluated multimodal imaging in the assessment of choroidal nevi and have found that fundus photography, spectral domain OCT, fundus AF, and ocular US all play an important role in the noninvasive detection of factors predictive of nevus growth into melanoma. We believe these features allow the clinician to objectively make a personalized judgement and share with the patient the potential risk of nevus growth into melanoma.

Key words: choroid, nevus, melanoma, transformation, growth, risk factors, multimodal imaging.

References

1. Shields JA, Shields CL. Intraocular Tumors. An Atlas and Textbook. 3rd ed. Philadelphia, PA: Lippincott Wolters Kluwers; 2016:69–80.
2. Shields CL, Shields JA, Kiratli H, et al. Risk factors for growth and metastasis of small choroidal melanocytic lesions. Ophthalmology 1995;102:1351–1361.
3. Shields CL, Cater JC, Shields JA, et al. Combination of clinical factors predictive of growth of small choroidal melanocytic tumors. Arch Ophthalmol 2000;118:360–364.
4. Shields CL, Furuta M, Berman EL, et al. Choroidal nevus transformation into melanoma. Analysis of 2514 consecutive cases. Arch Ophthalmol 2009;127; 981–987.
5. The Collaborative Ocular Melanoma Study Group. Factors predictive of growth and treatment of small choroidal melanoma. COMS report no. 5. Arch Ophthalmol 1997;115:1537–1544.
6. Singh AD, Mokashi AA, Bena JF, et al. Small choroidal melanocytic lesions. Features predictive of growth. Ophthalmology 2006;113:1032–1039.
7. Shields CL, Kaliki S, Hutchinson A, et al. Iris nevus growth into melanoma: analysis of 1611 consecutive eyes. The ABCDEF guide. Ophthalmology 2013;120:766–772.
8. Rigel DS, Friedman RJ, Kopf AW, Polsky D. ABCDE: an evolving concept in the early detection of melanoma. Arch Dermatol 2005;141:1032–1034.
9. Weinstock MA. Progress and prospects on melanoma: the way forward for early detection and reduced mortality. Clin Cancer Res 2006;12:2297s–2300s.
10. Riker AI, Sea N, Trinh T. The epidemiology, prevention, and detection of melanoma. Ochsner J 2010;10:56–65.
11. Schwartz JL, Wang TS, Hamilton TA, et al. Thin primary melanomas: associated detection patterns, lesion characteristics, and patient characteristics. Cancer 2002;95:1562–1568.
12. Kantor J, Kantor DE. Routine dermatologist-performed full-body skin examination and early melanoma detection. Arch Dermatol 2009;145:873–876.
13. Lindholm C, Andersson R, Dufmats M, et al. Invasive cutaneous malignant melanoma in Sweden, 1990-1999: a prospective, population-based study of survival and prognostic factors. Cancer 2004;101:2067–2078.
14. Pack GT, Lenson N, Gerber DM. Regional distribution of moles and melanomas. AMA Arch Surg 1952;65:862–870.
15. Eberhardt C, Percy SR, Branzan AL, et al. Early detection of skin cancer (EDISCIM) through the use of non-invasive confocal imaging. Stud Health Technol Inform 2004;103:279–286.
16. Elbaum M, Kopf AW, Rabinovitz HS, et al. Automatic differentiation of melanoma from melanocytic nevi with multispectral digital dermoscopy: a feasibility study. J Am Acad Dermatol 2001;44:207–218.
17. Butler P, Char DH, Zarbin M, Kroll S. Natural history of indeterminate pigmented choroidal tumors. Ophthalmology 1994;101:710–716.
18. Sumich P, Mitchell P, Wang JJ. Choroidal nevi in a white population: the Blue Mountains Eye Study. Arch Ophthalmol 1998;116:645–650.
19. Shields CL, Furuta M, Mashayekhi A, et al. Clinical spectrum of choroidal nevi based on age at presentation in 3422 consecutive eyes. Ophthalmology 2008;115:546–552.
20. Qiu M, Shields CL. Choroidal nevus in the United States adult population: racial disparities and associated factors in the National Health and Nutrition Examination Survey. Ophthalmology 2015;122:2071–2083.
21. Chien JL, Sioufi K, Surakiatchanukul T, et al. Choroidal nevus: a review of prevalence, features, genetics, risks, and outcomes. Curr Opin Ophthalmol 2017;28:228–237.
22. Espinoza G, Rosenblatt B, Harbour JW. Optical coherence tomography in the evaluation of retinal changes associated with suspicious choroidal melanocytic tumors. Am J Ophthalmol 2004;137:90–95.
23. Shields CL, Mashayekhi A, Materin MA, et al. Optical coherence tomography of choroidal nevus in 120 consecutive patients. Retina 2005;25:243–252.
24. Shields CL, Kaliki S, Rojanaporn D, et al. Enhanced depth imaging optical coherence tomography of small choroidal melanoma. Comparison with choroidal nevus. Arch Ophthalmol 2012;130:850–856.
25. Shields CL, Pellegrini M, Ferenczy SR, Shields JA. Enhanced depth imaging optical coherence tomography (EDI-OCT) of intraocular tumors. From placid to seasick to rock and rolling topography. The 2013 Francesco Orzalesi Lecture. Retina 2014;34:1495.
26. Shields CL, Bianciotto C, Pirondini C, et al. Autofluorescence of choroidal melanoma in 51 cases. Br J Ophthalmol 2008;92:617–622.
27. Shields CL, Pirondini C, Bianciotto C, et al. Autofluorescence of choroidal nevus in 64 cases. Retina 2008;28:1035–1043.